

The shape and simplicity biases of adversarially robust ImageNet-trained CNNs

Peijie Chen, Chirag Agarwal and Anh Nguyen*

ARTICLE INFO

Keywords:

Deep Learning
Computer Vision
Robustness
Adversarial Training
Interpretability
Texture vs. Shape

ABSTRACT

Increasingly more similarities between human vision and convolutional neural networks (CNNs) have been revealed in the past few years. Yet, vanilla CNNs often fall short in generalizing to adversarial or out-of-distribution (OOD) examples which humans demonstrate superior performance. Adversarial training is a leading learning algorithm for improving the robustness of CNNs on adversarial and OOD data; however, little is known about the properties, specifically the shape bias and internal features learned inside adversarially-robust CNNs. In this paper, we perform a thorough, systematic study to understand the shape bias and some internal mechanisms that enable the generalizability of AlexNet, GoogLeNet, and ResNet-50 models trained via adversarial training. We find that while standard ImageNet classifiers have a strong texture bias, their R counterparts rely heavily on shapes. Remarkably, adversarial training induces three simplicity biases into hidden neurons in the process of “robustifying” CNNs. That is, each convolutional neuron in R networks often changes to detecting (1) pixel-wise smoother patterns i.e. a mechanism that blocks high-frequency noise from passing through the network; (2) more lower-level features i.e. textures and colors (instead of objects); and (3) fewer types of inputs. Our findings reveal the interesting mechanisms that made networks more adversarially robust and also explain some recent findings e.g. why R networks benefit from much larger capacity (Xie and Yuille, 2020) and can act as a strong image prior in image synthesis (Santurkar et al., 2019).

1. Introduction

Convolutional neural networks (CNNs), specifically, AlexNet (Krizhevsky et al., 2012), have been increasingly found to exhibit interesting correspondences with human object recognition (Rajalingham et al., 2018; Serre, 2019; Cichy et al., 2016). However, a remarkable difference between ImageNet-trained CNNs and humans is that while the CNNs leverage mostly texture cues to categorize images, humans recognize an object by relying on its outline or silhouette (Geirhos et al., 2019). Interestingly, this shape bias of human vision was hypothesized to enable the superior performance of humans on out-of-distribution (OOD) data (Geirhos et al., 2018), which CNNs often misclassify.

For example, simply adding Gaussian noise to the input image can dramatically reduce AlexNet’s top-1 accuracy from ~57% to ~11% (Hendrycks and Dietterich, 2019). More severely, adding imperceptible, pixel-wise changes to an input image of a school bus yields a visually-identical image that would cause state-of-the-art CNNs to mislabel “ostrich” (Szegedy et al., 2014). An interesting class of CNNs that are state-of-the-art on such OOD noisy or adversarial data are adversarially-robust CNNs (hereafter, R networks), i.e. the networks that are trained to correctly label adversarial examples instead of real examples (Madry et al., 2018). That is, adversarial training has substantially improved model robustness to some types of out-of-distribution and adversarial data (Madry et al., 2018; Xie et al., 2020).

Therefore, we aim to understand the relationship between

the OOD performance and shape bias of R networks by answering three main questions. First, it remains unknown whether a *shape* bias exists in a R network trained on the large-scale ImageNet (Russakovsky et al., 2015), which often induces a large *texture* bias into vanilla CNNs (Geirhos et al., 2019), e.g. to separate ~150 four-legged species in ImageNet. Thus, an important question is:

Q1: *On ImageNet, do adversarially-robust networks (a.k.a., R networks) prefer shapes over textures?*

This question is interestingly also because Santurkar et al. (2019) found that ImageNet-trained R networks act as a strong image *texture* prior, i.e. they can be successfully used for many pixel-wise image optimization tasks.

Second, Geirhos et al. (2019) found that CNNs trained to be more *shape*-biased (but *not* via adversarial training) can generalize better to many unseen ImageNet-C (Hendrycks and Dietterich, 2019) image corruptions than S networks, which have a much weaker shape bias (Brendel and Bethge, 2019). Therefore, we ask:

Q2: *If an R network has a stronger preference for shapes than standard ImageNet-trained CNNs (hereafter, S networks), will it perform better on OOD images?*

It is worth noting that R networks, which were trained solely on adversarial examples, often *underperform* S networks on real test sets (Tsipras et al., 2019). Beside being more robust to adversarial attacks, some CNNs trained via AdvProp (Xie et al., 2020) (a variant of Madry et al. (2018)’s adversarial training framework that trains CNNs on both real and adversarial data) obtain a similarly high accuracy on real data as S networks; however, it is unknown whether AdvProp CNNs are shape- or texture-biased (which we answer in Table 2).

Third, while most prior work studied the behaviors of R CNNs as a black-box classifier, little is known about the internal network characteristics of R networks and, what en-

*Corresponding author.

All authors from Auburn University.

✉ peijie.chen.auburn@gmail.com (P. Chen);

chirag.agarwal112@gmail.com (C. Agarwal); anh.ng8@gmail.com (A. Nguyen)

ORCID(s):

able their shape bias and OOD performance. Therefore, we attempt to shed light into the last question:

Q3: *How did adversarial training change the hidden neural representations to make CNNs more shape-biased and adversarially-robust?*

In this paper, we harness two common datasets in ML interpretability and neuroscience—cue-conflict (Geirhos et al., 2019) and NetDissect (Bau et al., 2017)—to answer the three questions above via a systematic study across three different convolutional architectures—AlexNet (Krizhevsky et al., 2012), GoogLeNet (Szegedy et al., 2015), and ResNet-50 (He et al., 2016)—trained to perform image classification on the large-scale ImageNet dataset (Russakovsky et al., 2015). We find that:¹

1. R classifiers trained on ImageNet prefer shapes over textures ~67% of the time—a stark contrast to S classifiers, which prefer shapes at ~25% (Sec. 3.1).
2. Consistent with the strong shape bias, R classifiers interestingly outperform S counterparts on texture-less, distorted images (stylized and silhouetted images) (Sec. 3.2.2).
3. Adversarial training makes CNNs more robust by (a) blocking pixel-wise input noise via smooth filters (Sec. 3.3.1), (b) reducing the set of high-activating inputs to simple patterns (Sec. 3.3.2).
4. Units that detect texture patterns (according to NetDissect) are not only useful to texture-based image classification but can be also highly useful to *shape*-based classification (Sec. 3.4).
5. By aligning NetDissect and cue-conflict frameworks, we found that hidden neurons in R networks are surprisingly neither strongly shape-biased nor texture-biased, but instead generalists that detect low-level features (Sec. 3.4).

The exciting differences between human vision and R CNNs revealed by our work can inform future research into what enables the strong generalization capability of human vision and how to improve state-of-the-art CNNs.

2. Networks and Datasets

Networks To understand the effects of adversarial training across a wide range of architectures, we compare each pair of S and R models while keeping their network architectures constant. That is, we conduct all experiments on two groups of classifiers: (a) standard AlexNet, GoogLeNet, & ResNet-50 (hereafter, ResNet) models pre-trained on the 1000-class 2012 ImageNet dataset; and (b) three adversarially-robust counterparts i.e. AlexNet-R, GoogLeNet-R, & ResNet-R which were trained via adversarial training (see below).

Training A standard classifier with parameters θ was trained to minimize the cross-entropy loss L over pairs of (training example x , ground-truth label y) drawn from the ImageNet training set \mathcal{D} :

$$\arg \min_{\theta} \mathbb{E}_{(x,y) \sim \mathcal{D}} [L(\theta, x, y)] \quad (1)$$

¹All code and data will be available on github upon publication.

On the other hand, we trained each R classifier via Madry et al. (2018) adversarial training framework where each real example x is changed by a perturbation Δ :

$$\arg \min_{\theta} \mathbb{E}_{(x,y) \sim \mathcal{D}} \left[\max_{\Delta \in \mathcal{P}} L(\theta, x + \Delta, y) \right] \quad (2)$$

and \mathcal{P} is the perturbation range allowed within an L_2 norm.

Hyperparameters The S models were downloaded from PyTorch model zoo (PyTorch, 2019). We adversarially trained all R models using the robustness library (Engstrom et al., 2019), using *the same* hyperparameters in (Engstrom et al., 2020; Santurkar et al., 2019; Bansal et al., 2020) because these previous works have shown that adversarial training significantly changed the inner-workings of ImageNet CNNs—i.e. becoming a strong image prior with perceptually-aligned deep features. That is, adversarial examples were generated using Projected Gradient Descent (PGD) (Madry et al., 2018) with an L_2 norm constraint ϵ of 3, a step size of 0.5, and 7 PGD-attack steps. R models were trained using an SGD optimizer for 90 epochs with a momentum of 0.9, an initial learning rate of 0.1 (which is reduced 10 times every 30 epochs), a weight decay of 10^{-4} , and a batch size of 256 on 4 Tesla-V100 GPU's.

Compared to the standard counterparts, R models have substantially higher adversarial accuracy but lower ImageNet validation-set accuracy (Table 1). To compute adversarial accuracy, we perturbed validation-set images with the same PGD attack settings as used in training.

Correctly-labeled image subsets: ImageNet-CL Following Bansal et al. (2020), to compare the behaviors of two networks of identical architectures on the same inputs, we tested them on the largest ImageNet validation subset (hereafter, ImageNet-CL) where both models have 100% accuracy. The sizes of the three subsets for three architectures—AlexNet, GoogLeNet, and ResNet—are respectively: 17,693, 20,238, and 27,343. On modified ImageNet images (e.g., adversarial in Fig. 1b), we only tested each CNN pair on the modified images whose original versions exist in ImageNet-CL. That is, we wish to gain deeper insights into how CNNs behave on correctly-classified images, and then how their behaviors change when some input feature (e.g. textures or shapes) is modified.

3. Experiment and Results

3.1. Do ImageNet adversarially-robust networks prefer shapes or textures?

It is important to know which input feature a classifier uses when making decisions. While standard ImageNet networks often carry a strong texture bias (Geirhos et al., 2019), it is unknown whether their adversarially-robust counterparts would be heavily texture- or shape-biased. Here, we test this hypothesis by comparing S and R models on the well-known cue-conflict dataset (Geirhos et al., 2019). That is, we feed “stylized” images provided by Geirhos et al. (2019) that contain contradicting texture and shape cues (e.g. elephant skin on a cat silhouette) and count the times a model uses textures

Table 1

Top-1 accuracy (%) on 50K-image ImageNet validation-set and PGD adversarial images (number of iterations = 7; $\epsilon = 3$; step size = 0.5).

Architecture	AlexNet		GoogLeNet		ResNet-50			
Training algorithm	Standard	Robust	Standard	Robust	Standard	AdvProp PGD1	AdvProp PGD5	Robust
ImageNet	56.52	39.83	69.78	43.57	76.13	77.31	77.01	57.90
Adversarial	0.18	22.27	0.08	31.23	0.35	69.02	73.55	36.11

Table 2

While Standard classifiers rely heavily on textures, Robust classifiers rely heavily on shapes. Texture and Shape bias scores are the top-1 accuracy (%) computed on the cue-conflict dataset proposed by Geirhos et al. (2019).

Architecture	AlexNet		GoogLeNet		ResNet-50			
Training algorithm	Standard	Robust	Standard	Robust	Standard	AdvProp PGD1	AdvProp PGD5	Robust
Training data	Real	Adv.	Real	Adv.	Real	Real + Adv.	Real + Adv.	Adv.
Texture	73.61	34.67	74.91	34.43	77.79	68.24	63.11	29.63
Shape	26.39	65.32	25.08	65.56	22.20	31.75	36.89	70.36

or shapes (i.e. outputting elephant or cat) when it makes a correct prediction.

Experiment Our procedure follows Geirhos et al. (2019). First, we excluded 80 images that do not have conflicting cues (e.g. cat textures on cat shapes) from their 1,280-image dataset. Each texture or shape cue belongs to one of 16 MS COCO (Caesar et al., 2018) coarse labels (e.g. cat or elephant). Second, we ran the networks on these images and converted their 1000-class probability vector outputs into 16-class probability vectors by taking the average over the probabilities of the fine-grained classes that are under the same COCO label. Third, we took only the images that each network correctly labels (i.e. into the texture or shape class), which ranges from 669 to 877 images (out of 1,200) for 6 networks and computed the texture and shape accuracies over 16 classes.

Results On average, over three architectures, R classifiers rely on shapes $\geq 67.08\%$ of the time, i.e. $\sim 2.7\times$ higher than 24.56% of the S models (Table 2). In other words, by replacing real with adversarial examples, adversarial training causes the heavy texture bias of ImageNet classifiers (Geirhos et al., 2019; Brendel and Bethge, 2019) to drop substantially ($\sim 2.7\times$). Additionally, we also test two adversarially-robust models that are trained on a mix of real and adversarial data via AdvProp (Xie et al., 2020) with a PGD $L_2 \epsilon$ of 1 and 5, respectively (see full hyperparameters in the training code). These AdvProp models obtain a similarly high accuracy on both validation as well as adversarial images (Table 1; PGD1 & PGD5). Interestingly, AdvProp models are also heavily texture-biased (Table 2; 68.24% vs. 31.75%) but their preferences are in between that of the vanilla and R models. Moreover, as CNNs are trained with increasingly more adversarial perturbations and less real data (from Standard \rightarrow PGD1 \rightarrow PGD5 \rightarrow Robust), the texture bias also decreases (from

$77.79\% \rightarrow 68.24\% \rightarrow 63.11\% \rightarrow 29.63\%$; Table 2). This result presents a strong evidence that **real ImageNet images strongly induce a texture bias** and **adversarial images induce a shape bias** into CNNs.

3.2. Do robust networks generalize to unseen types of distorted images?

Geirhos et al. (2019) found that some training regimes that encourage CNNs to focus more on *shape* can improve their performance on unseen image distortions. Sec. 3.1 shows that training with more adversarial examples makes a CNN more shape-biased. Therefore, it is interesting here to understand how adversarial training improves CNN generalization performance.

That is, we test R models on two types of *controlled* images where either shape or texture cues are removed from the original, correctly-labeled ImageNet images (Fig. 1c–f). Note that when both shape and texture cues are present, e.g. in cue-conflict images, R classifiers consistently prefer shape over texture, i.e. a *shape bias* (Table 2). However, this bias may not necessarily carry over to the images where only either texture or shape cues are present.

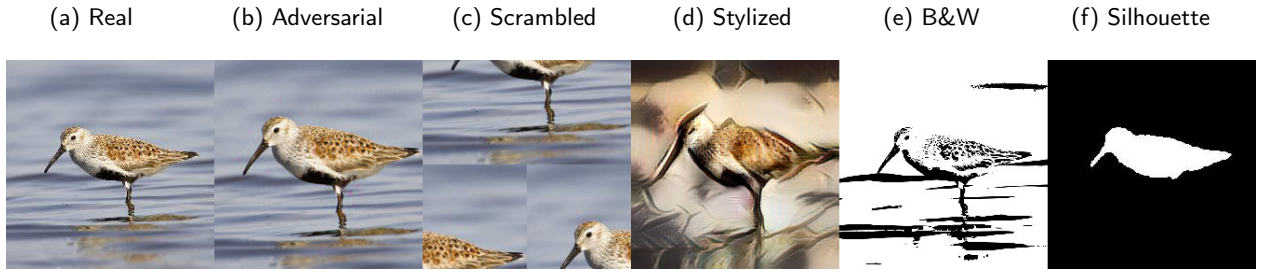
3.2.1. Performance on shape-less images

We create shape-less images by dividing each ImageNet-CL image into a grid of $p \times p$ even patches where $p \in \{2, 4, 8\}$ and re-combining them randomly into a new “scrambled” version (Fig. 1c). On average, over three grid types, we observed a larger accuracy drop in R models compared to S models, ranging from $1.6\times$ to $2.04\times$ lower accuracy (Table 3d). That is, **R models become substantially less accurate than S models when shape cues are removed by patch-shuffling**—another evidence for their exclusive reliance on shapes (instead of textures). See Fig. 2 for the predictions of ResNet and ResNet-R on scrambled patches.

Table 3

Adversarially-robust (R) models outperform vanilla (S) models when both are under PGD-adversarial attacks (b). R models consistently outperform S model in texture-less (e,f) distortions. Here, we report top-1 accuracy scores (%) on the transformed images whose original real versions were correctly-labeled (a) by both S and R models. “Scrambled” column (c) shows the mean accuracy scores over three patch-scrambling types (details in Fig. 3).

Network	(a) Real ImageNet	(b) Adversarial	Shape-less	Texture-less		
			(c) Scrambled	(d) Stylized	(e) B&W	(f) Silhouette
AlexNet	100	0.18	34.59	6.31	20.08	7.72
AlexNet-R	100	22.27	16.92	9.11	35.25	9.30
GoogLeNet	100	0.08	49.74	13.74	43.48	10.17
GoogLeNet-R	100	31.23	31.15	12.54	44.55	24.12
ResNet	100	0.35	58.04	10.68	16.96	3.95
ResNet-R	100	36.11	34.46	15.62	53.89	22.30

**Figure 1:** Example distorted images (b–g). See Fig. A5 for more examples.

3.2.2. Performance on texture-less images

Following Geirhos et al. (2019), we test R models on three types of texture-less images where the texture is increasingly removed: (1) stylized ImageNet images where textures are randomly modified; (2) binary, black-and-white, i.e. B&W, images (Fig. 1e); and (3) silhouette images where the texture information is completely removed (Fig. 1f).

Stylized ImageNet To construct a set of stylized ImageNet images (see Fig. 1d), we take all ImageNet-CL images (Sec. 2) and change their textures via a stylization procedure in Geirhos et al. (2019), which harnesses the style-transfer technique (Gatys et al., 2016) to apply a random style to each ImageNet “content” image.

B&W images For all ImageNet-CL images, we use the same process described in Geirhos et al. (2019) to generate silhouettes, but we do not manually select or modify the images. We use ImageMagick (2020) to binarize ImageNet images into B&W images via the following steps:

```
convert image.jpeg image.bmp
potrace -svg image.bmp -o image.svg
rsvg-convert image.svg > image.jpeg
```

Silhouette For all ImageNet-CL images, we obtain their segmentation maps via a PyTorch DeepLab-v2 model (Chen et al., 2017) pre-trained on MS COCO-Stuff. We used the ImageNet-CL images that belong to a set of 16 COCO superclasses in Geirhos et al. (2019) (e.g. bird, bicycle, airplane). When evaluating classifiers, an image is considered correctly

labeled if its ImageNet predicted label is a subclass of the correct COCO superclass (Fig. 1f; sandpiper → bird).

Results Consistently, **on all three texture-less image sets, R models outperformed their S counterparts** (Table 3d–f)—a remarkable generalization capability, especially on B&W and silhouette images where little to no texture information is available.

3.3. What internal mechanisms make adversarially trained CNNs more robust than standard CNNs?

We have shown that after adversarial training, R models are more robust than S models on new adversarial examples generated for these pre-trained models via PGD attacks (Table 3b). Furthermore, on non-adversarial, high-frequency images, R models may also outperform S models (Table A1a; AlexNet-R) (Yin et al., 2019; Gilmer et al., 2019).

We aim to understand the internal mechanisms that make R CNNs more robust to high-frequency noise by analyzing the networks at the weight (Sec. 3.3.1) and neuron (Sec. 3.3.2) levels.

3.3.1. Weight level: Smooth filters to block pixel-wise noise

Smoother filters To explain this phenomenon, we visualized the weights of all 64 conv1 filters (11×11×3), in both AlexNet and AlexNet-R, as RGB images. We compare each AlexNet conv1 filter with its nearest conv1 filter (via Spear-

Biases in Adversarially Robust CNNs

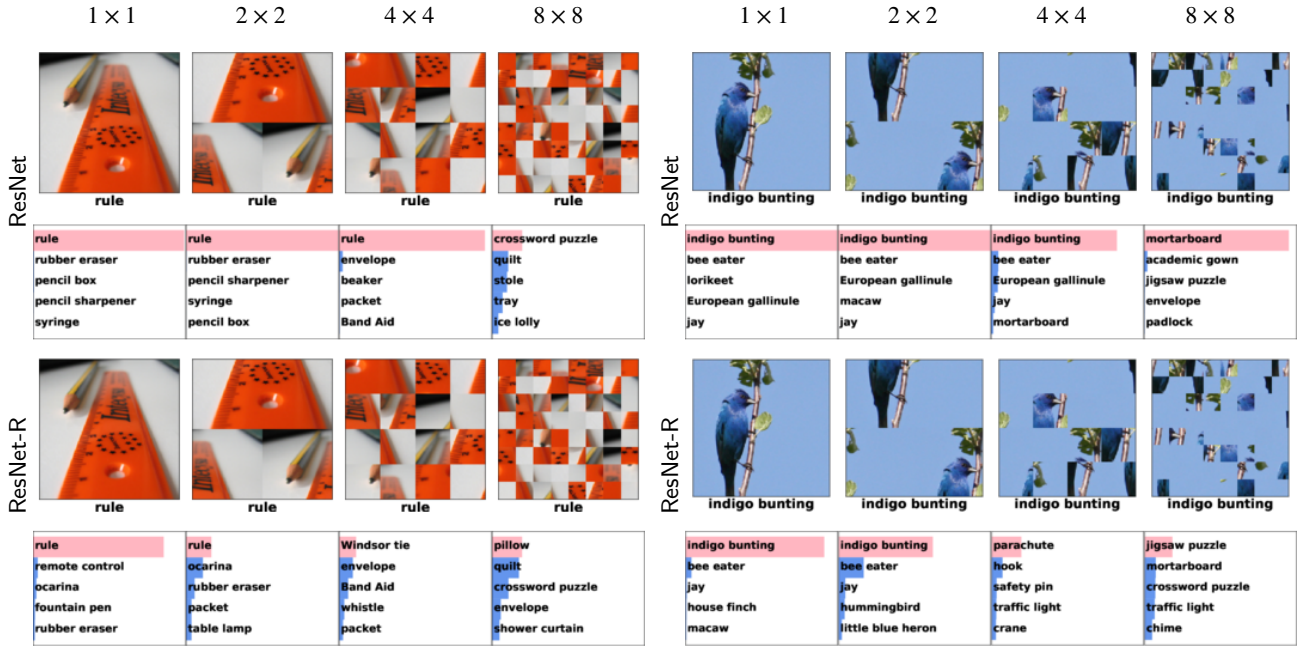


Figure 2: Qualitative examples showing the strong *texture* bias of standard CNNs (here, ResNet) and the strong *shape* bias of adversarially-robust models (here, ResNet-R) as described in Sec. 3.2.1. When patches are scrambled, ResNet-R confidence drops substantially and its **top-1 predicted** labels often change away from the original, correctly-predicted label, here, rule (left) and indigo bunting (right).

Table 4

Mean total variation (TV) of the conv layers of 6 models.

	AlexNet	AlexNet-R	GoogLeNet	GoogLeNet-R	ResNet	ResNet-R
Mean TV	110.20	63.59	36.53	22.79	18.35	19.96

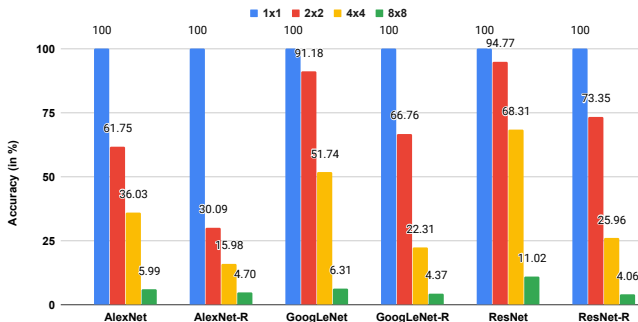


Figure 3: Standard CNNs substantially outperform R models on scrambled versions of the ImageNet-CL images due to their capability of recognizing images using textures. Here, we report top-1 accuracy (%) on the scrambled images whose original versions (ImageNet-CL) were correctly-labeled by both standard and R classifiers (hence, the 100% for 1×1 blue bars).

man rank correlation) in AlexNet-R. Remarkably, R filters appear qualitatively much smoother than their counterparts (Fig. 4a). The R filter bank is also less diverse, e.g. R edge detectors are often black-and-white in contrast to the color-

ful AlexNet edges (Fig. 4b). A similar contrast was also seen for the GoogLeNet and ResNet models (Fig. A1).

We also quantify the smoothness, in total variation (TV) (Rudin et al., 1992), of the filters of all 6 models (Table 4) and found that, on average, the filters in R networks are much smoother.

For example, the mean TV of GoogLeNet-R is about 1.5 times smaller than that of GoogLeNet.

In almost all layers, R filters are smoother than S filters (Fig. A9).

Blocking pixel-wise noise

We hypothesize that the smoothness of filters makes R classifiers more robust against noisy images.

To test this hypothesis, we computed the total variation of the channels across 5 conv layers when feeding ImageNet-CL images and their noisy versions (Fig. 1c; ImageNet-C Level 1 additive noise $\sim N(0, 0.08)$) to S and R models.

At conv1, the smoothness of R activation maps remains almost unchanged before and after noise addition (Fig. 5a;

yellow circles are on the diagonal line). In contrast, the conv1 filters in standard AlexNet allow Gaussian noise to pass through, yielding larger-TV channels (Fig. 5a; blue cir-

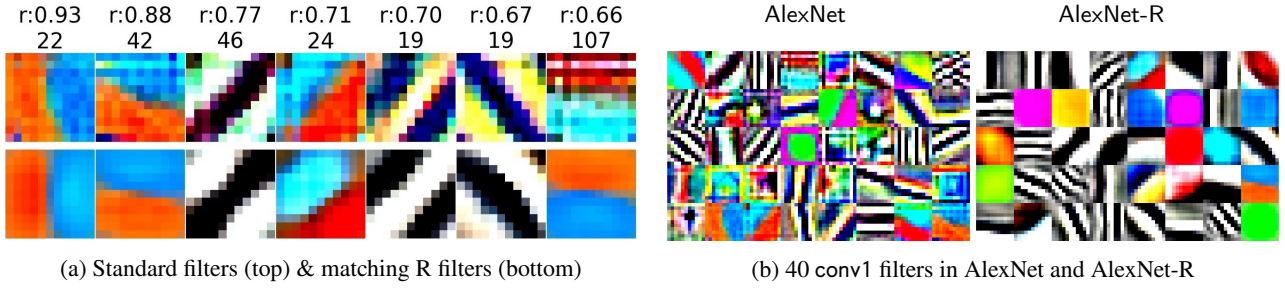


Figure 4: **Left:** For each AlexNet conv1 filter (top row), we show the highest-correlated filter in AlexNet-R (bottom row), their Spearman rank correlation (e.g. $r: 0.93$) and the Total Variation (TV) difference (e.g. 22) between the top kernel and the bottom. Here, the TV differences are all positive i.e. AlexNet filters have higher TV. See Fig. A2 for full plot. **Right:** conv1 filters of AlexNet-R are smoother and less diverse than the counterparts. See Figs. A1 for GoogLeNet & ResNet.

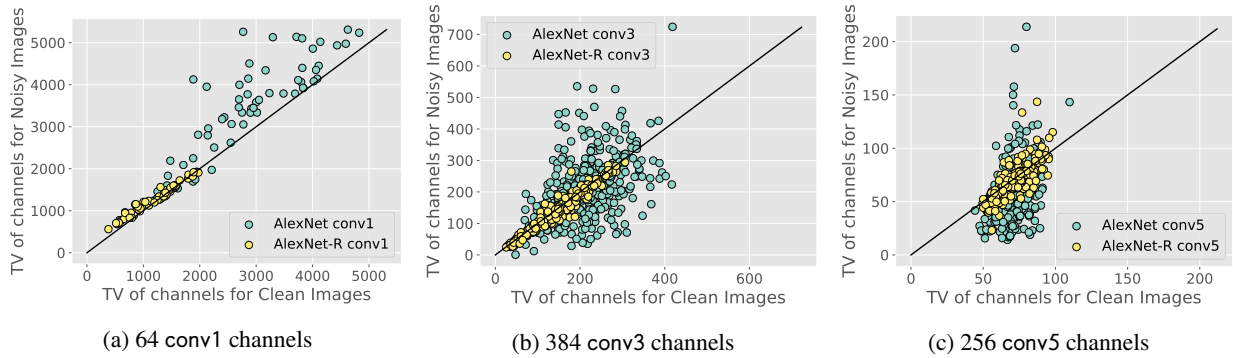


Figure 5: In each subpanel, one point shows the mean Total Variation (TV) of one channel when running clean ImageNet-CL images and their noisy versions through AlexNet (●) or AlexNet-R (●). R channels have similar TV before and after adding noise, suggesting that conv1 kernels filter out the added noise. In higher layers (conv3 and conv5), R channels are consistently more invariant to the input noise than S channels (● dots are clustered around the diagonal line while ● dots have higher variance). See Fig. A4 for the same scatter plot (a) for all five layers.

cles are mostly above the diagonal). That is, the smooth filters in **R models indeed can filter out pixel-wise Gaussian noise despite that R models were not explicitly trained on this image type!** Furthermore, AlexNet-R and ResNet-R consistently perform better in different noise distortions (Table A1 (a)) compared to their S models.

In higher layers, it is intuitive that the pixel-wise noise added to the input image might not necessarily cause activation maps, in both S and R networks, to be noisy because higher-layered units detect more abstract concepts. However, interestingly, we still found that R channels to have consistently less mean TV (Fig. 5b–c).

Our result suggests that most of the de-noising effects take place at lower layers (which contain more generic features) instead of higher layers (which contain more task-specific features).

3.3.2. Neuron level: Robust neurons prefer lower-level and fewer inputs

Here, via NetDissect framework, we wish to characterize how adversarial training changed the hidden neurons in R

networks to make R classifiers more adversarially robust.

Network Dissection (hereafter, NetDissect) is a common framework for quantifying the functions of a neuron by computing the Intersection over Union (IoU) between each activation map (i.e. channels) and the human-annotated segmentation maps for the same input images.

That is, each channel is given an IoU score per human-defined concept (e.g. *dog* or *zigzagged*) indicating its accuracy in detecting images of that concept. A channel is tested for its accuracy on all $\sim 1,400$ concepts,

which span across six coarse categories: *object*, *part*, *scene*, *texture*, *color*, and *material* (Bau et al., 2017) (c.f. Fig. A11 for example NetDissect images in *texture* and *color* concepts).

Following Bau et al. (2017), we assign each channel C a main functional label i.e. the concept that C has the highest IoU with. In both S and R models, we ran NetDissect on all 1152, 5808, and 3904 channels from, respectively, 5, 12, and 5 main convolutional layers (post-ReLU) of the AlexNet, GoogLeNet, and ResNet-50 architectures (c.f. Sec. A for more details of layers used).

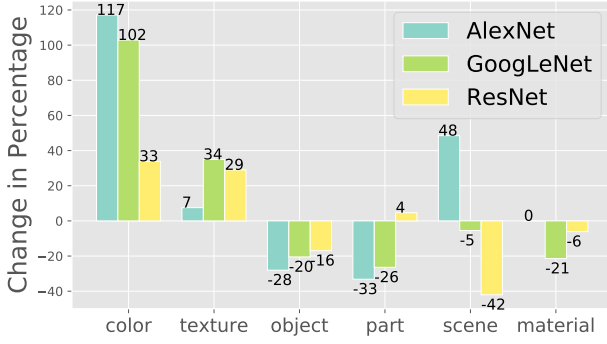


Figure 6: Total channel increases (%) in R models. For all three architectures, the numbers of NetDissect color and texture detectors in R models increase, e.g. by 117% and 7%, respectively, for AlexNet, while the number of object units decreases by 28%. See Fig. A3 for layer-wise plots for AlexNet in other object and color category.

Shift to detecting more low-level features i.e. colors and textures We found a consistent trend—adversarial training resulted in substantially more filters that detect colors and textures (i.e. in R models) in exchange for fewer object and part detectors.

For example, throughout the same GoogLeNet architecture, we observed a 102% and a 34% increase of color and texture detectors, respectively, in the R model, but a 20% and a 26% fewer object and part detectors, compared to the S model (c.f. Fig. 6). After adversarial training, ~11%, 15%, and 10% of all hidden neurons (in the tested layers) in AlexNet, GoogLeNet, and ResNet, respectively, shift their roles to detecting lower-level features (i.e. textures and colors) instead of higher-level features (see feature visualizations in Fig. 10).

Across three architectures, the increases in texture and color channels are often larger in higher layers. The largest functional shifts appearing in higher layers can be because the higher-layered units are more task-specific (Nguyen et al., 2016a; Yosinski et al., 2014).

Consistent findings with ResNet CNNs trained on Stylized ImageNet We also compare the shape-biased ResNet-R with ResNet-SIN, i.e. a ResNet-50 trained exclusively on stylized ImageNet images where textures are removed via stylization (Geirhos et al., 2019). ResNet-SIN also has a strong shape bias of 81.37%.² Interestingly, similar to ResNet-R, ResNet-SIN also has more low-level feature detectors (colors and textures) and fewer high-level feature detectors (objects and parts) than the vanilla ResNet (Fig. 7). In contrast, finetuning this ResNet-SIN on ImageNet remarkably changes the model to be *texture-biased* (at a 79.7% texture bias) and to contain fewer texture and more object and part units (Fig. 7; ResNet-SIN+IN vs. ResNet-SIN).

That is, training or finetuning on ImageNet tend to cause CNNs to be more texture-biased and contain more high-level features (i.e. detecting objects and parts). In contrast, train-

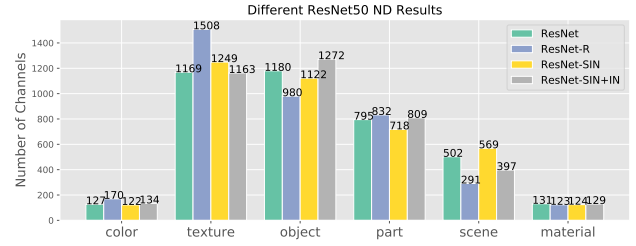


Figure 7: Each column shows the number of channels (in a ResNet-50 model) categorized into one of NetDissect categories. For example, the standard ImageNet-trained ResNet has 127 color detectors (leftmost column). Here, we compare the neural functions among four different ResNet-50 models trained differently: (1) ResNet was trained on ImageNet; (2) ResNet-R was trained via PGD-adversarial training; (3) ResNet-SIN was trained on texture-removed ImageNet from (Geirhos et al., 2019); and (4) ResNet-SIN+IN was a ResNet-SIN that was then finetuned on ImageNet. Training on texture-removed ImageNet or adversarial examples consistently produces CNNs that are (a) heavily shape-biased; (b) contain more low-level, texture features; (c) fewer high-level, object detectors compared to training on ImageNet which produces texture-biased CNNs (ResNet and ResNet-SIN+IN).

ing on adversarial examples or texture-distorted images cause CNNs to focus more on shapes and learn more generic, low-level features.

Shift to detecting simpler objects Analyzing the concepts in the object category where we observed largest changes in channel count, we found evidence that neurons change from detecting complex to simpler objects. That is, for each NetDissect concept, we computed the difference in the numbers of channels between the S and R model. In the same object category, AlexNet-R model has substantially fewer channels detecting complex concepts e.g. -30 dog, -13 cat, and -11 person detectors (Fig. A10b; rightmost columns), compared to the standard network. In contrast, the R model has more channels detecting simpler concepts, e.g. +40 sky and +12 ceiling channels (Fig. A10b; leftmost columns). The top-49 images that highest-activated R units across five conv layers also show their strong preference for simpler backgrounds and objects (Fig. 10).

Shift to detecting fewer unique concepts The previous sections have revealed that neurons in R models often prefer images that are pixel-wise smoother (Sec. 3.3.1) and of lower-level features (Sec. 3.3.2), compared to S neurons. Another important property of the complexity of the function computed at each neuron is the diversity of types of inputs detected by the neuron (Nguyen et al., 2016b, 2019). Here, we compare the diversity score of NetDissect concepts detected by units in S and R networks. For each channel C , we calculated a diversity score, i.e. the number of unique concepts that C detects with an IoU score ≥ 0.01 .

Interestingly, on average, an R unit fires for 1.16 times

²model_A in <https://github.com/rgeirhos/texture-vs-shape/>. See Table 4 in Geirhos et al. (2019).

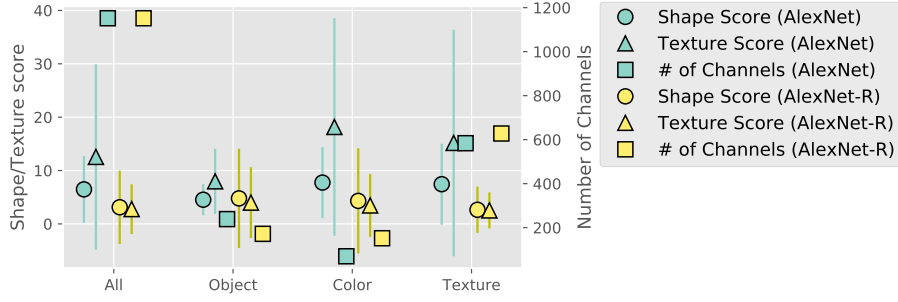


Figure 8: Shape & Texture score of AlexNet & AlexNet-R. The average Shape (●) and Texture (▲) scores over all channels in the entire network (“All”) or in a NetDissect category (“Object”, “Color”, and “Texture”). While AlexNet-R has more color and texture channels (■ above ■), these R channels are not heavily shape- or texture-biased. In contrast, the corresponding channels in AlexNet are heavily texture-biased (▲ is almost 2× of ●).

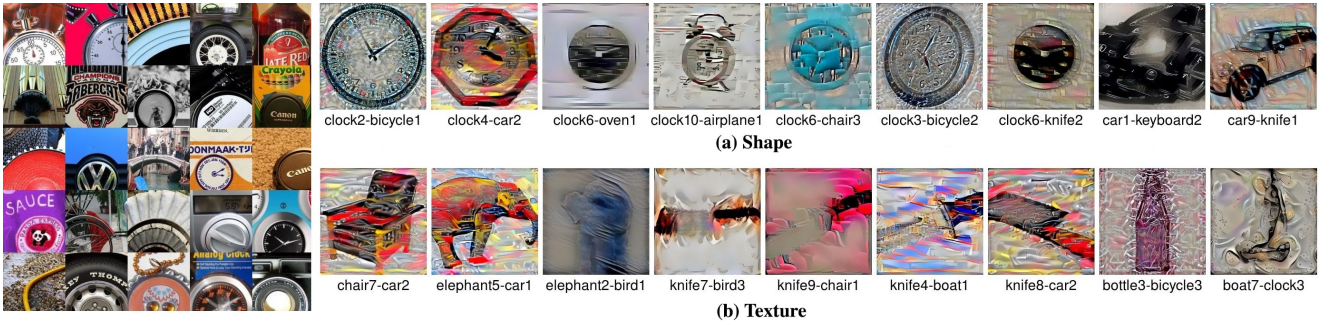


Figure 9: Left: Top-25 highest-activation images of the AlexNet unit conv4₁₉, which has a NetDissect label of spiralled under texture category. The unit prefers circular patterns including car wheels and clock. Right: Example *cue-conflict* images originally labeled by AlexNet as shape (top) or texture (bottom) but that were given a different label after the unit conv4₁₉ is ablated. For example, “clock2-bicycle1” is a cue-conflict image that has the shape of a clock and the texture of a bicycle. Qualitatively, the unit helps AlexNet detect clocks and cars using shapes (top) and reddish pink cars, birds, chairs, and bicycles using textures (bottom). The unit has Shape and Texture scores of 18 and 22, respectively. See Fig. A6 & Fig. A7 for more examples.

fewer unique concepts than an S unit (22.43 vs. 26.07; c.f. Fig. A12a). Similar trends were observed in ResNet (Fig. A12b). Qualitatively comparing the highest-activation training-set images by the highest-IoU channels in both networks, for the same most-frequent concepts (e.g. striped), often confirms a striking difference: R units prefer a less diverse set of inputs (Fig. 10). As R hidden units fire for fewer concepts, i.e. significantly fewer inputs, the space for adversarial inputs to cause R models to misbehave is strictly smaller.

3.4. Which neurons are important for shape-based or texture-based image classification?

To understand how the found changes in R neurons (Sec. 3.3) relate to the shape bias of R CNNs (Sec. 3.1), here, we zero out every channel, one at a time, in S and R networks and measure the performance drop in recognizing shapes and textures from cue-conflict images.

Shape & Texture scores For each channel, we computed a “Shape score”, i.e. the number of images originally correctly labeled into the shape class by the network but that, after

the ablation, are labeled differently (examples in Fig 9a–b). Similarly, we computed a Texture score per channel. The Shape and Texture scores quantify the importance of a channel in image classification using shapes and textures, respectively.

First, we found that the **channels labeled texture by NetDissect are not only important to texture-based but also shape-based classification**. That is, on average, zero-ing out these channels caused non-zero Texture and Shape scores (Fig. 8; Texture ● and ▲ are above 0). See Fig. 9 for an example of texture channels with high Shape and Texture scores.

This result is aligned with the fact that R networks consistently have more texture units (Fig. 6) but are shape-biased (Sec. 3.1).

Second, the texture units are, as expected, highly texture-biased in AlexNet (Fig. 8 Texture; ▲ is almost 2× of ●). However, surprisingly, those texture units in AlexNet-R are **neither strongly shape-biased nor texture-biased** (Fig. 8; Texture ● ≈ ▲). That is, across all three groups of the object,

color, and texture, **R neurons appear mostly to be generalist, low-level feature detectors.** This generalist property might be a reason for why R networks are more effective in transfer learning than S networks (Salman et al., 2020).

Finally, the contrast above between the texture bias of S and R channels (Fig. 8) reminds researchers that the single semantic label assigned by NetDissect to each neuron is not describing a full picture of what the neuron does and how it helps in downstream tasks. To the best of our knowledge, this is the first work to align the NetDissect and cue-conflict frameworks to study how individual neurons contribute to the generalizability and shape bias of the entire network.

4. Related Work

Shape bias On smaller-scaled datasets e.g. CIFAR-10, Zhang and Zhu (2019) also found that R networks rely heavily on shapes (instead of textures) to classify images. However, such shape bias may not necessarily generalize to high-dimensional, large-scale datasets such as ImageNet. Different from Zhang and Zhu (2019), here, we study networks trained on ImageNet and its variants (e.g. Stylized ImageNet). To the best of our knowledge, we are the first to reveal (1) the shape bias of ImageNet-trained R networks; (2) the roles of neurons in R networks; and (3) their internal robustification mechanisms. We also found that our adversarially-trained CNNs and the CNNs trained on texture-removed images by Geirhos et al. (2019) both similar have a strong shape bias and contain simpler and more generic features than standard ImageNet-trained CNNs.

Simplicity bias Deep neural networks tend to prioritize learning simple patterns that are common across the training set (Arpit et al., 2017). Furthermore, deep ReLU networks often prefer learning simple functions (Valle-Perez et al., 2019; De Palma et al., 2019), specifically low-frequency functions (Rahaman et al., 2019), which are more robust to random parameter perturbations. Along this direction, here, we have shown that R networks (1) have smoother weights (Sec. 3.3.1), (2) prefer even simpler and fewer inputs (Sec. 3.3.2) than standard deep networks—i.e. R networks represent even simpler functions. Such simplicity biases are consistent with the fact that gradient images of R networks are much smoother (Tsipras et al., 2019) and that R classifiers act as a strong image prior for image synthesis (Santurkar et al., 2019).

Robustness Each R neuron computing a more restricted function than an S neuron (Sec. 3.3.2) implies that R models would require more neurons to mimic a complex S network. This is consistent with recent findings that adversarial training requires a larger model capacity (Xie and Yuille, 2020). In Sec. 3.3.1, we found that adversarial training produces network that are robust to images with additive Gaussian noise. Interestingly, Ford et al. (2019) found the reverse is also true: Training CNNs with additive Gaussian noise can improve the performance on adversarial examples.

While AdvProp did not yet show benefits on ResNet (Xie et al., 2020), it might be interesting future work to find out whether EfficientNets trained via AdvProp also have shape

and simplicity biases. Furthermore, simplicity biases may be incorporated as regularizers into future training algorithms to improve model robustness. For example, encouraging filters to be smoother might improve robustness to high-frequency noise.

Also aligned with our findings, Rozsa and Boulton (2019) found that explicitly narrowing down the non-zero input regions of ReLUs can improve adversarial robustness.

5. Discussion and Conclusion

We found that R networks heavily rely on shape cues in contrast to S networks. One may fuse an S network and a R network (two channels, one uses texture and one uses shape) into a single, more robust, interpretable ML model. That is, such model may (1) have better generalization on OOD data than S or R network alone and (2) enable an explanation to users on what features a network uses to label a given image.

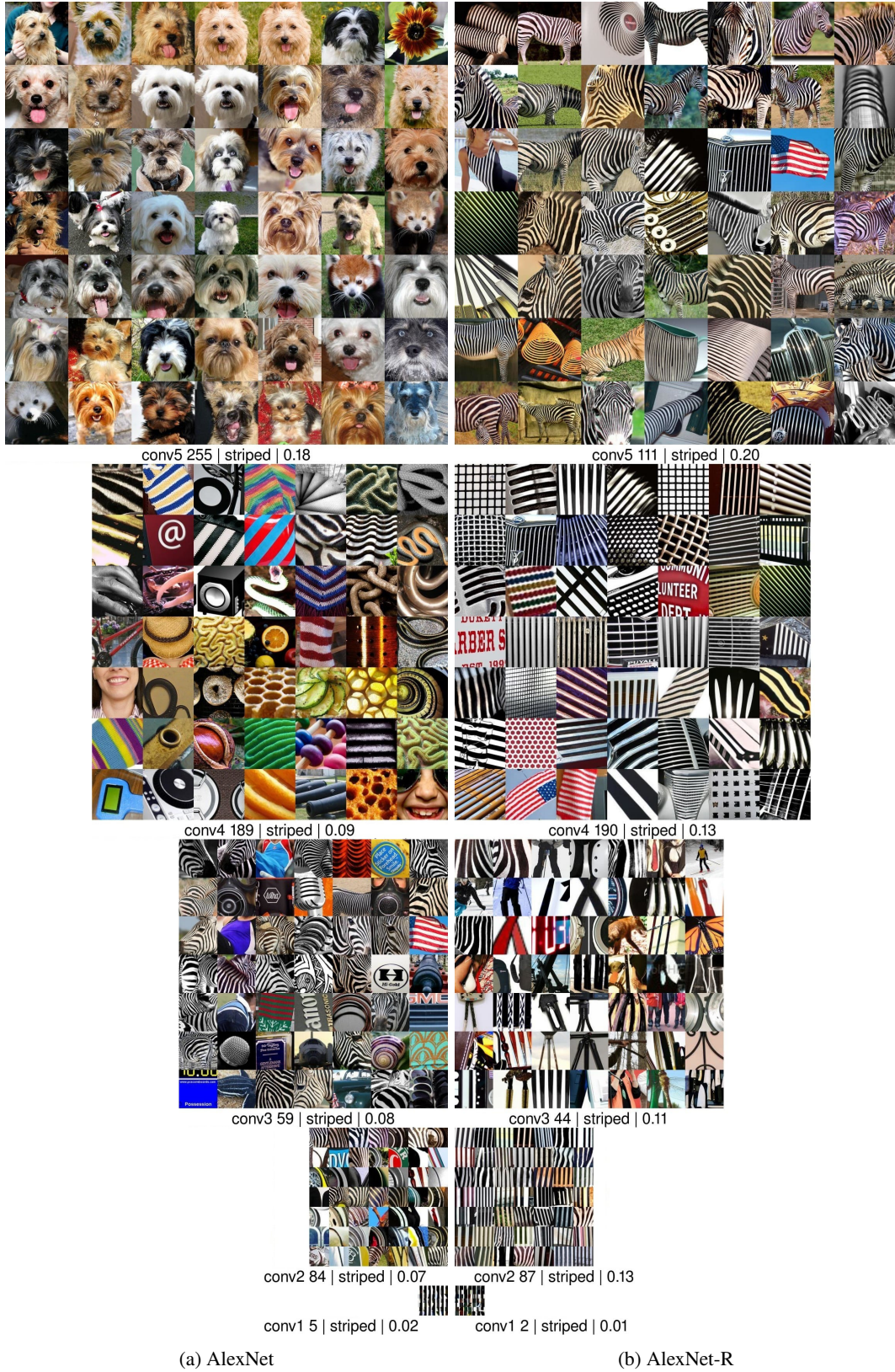
Our study on how individual hidden neurons contribute to the R network shape preference (Sec. 3.4) revealed that texture-detector units are equally important to the texture-based and shape-based recognition. This is in contrast to a common hypothesis that texture detectors should be exclusively only useful to texture-biased recognition. Our surprising finding suggests that the categories of stimuli in the well-known Network Dissection (Bau et al., 2017) need to be re-labeled and also extended with low-frequency patterns e.g. single lines or silhouettes in order to more accurately quantify hidden representations.

It might be interesting future work to improve model performance by (1) training them jointly on adversarial examples and texture-less images; and (2) adding smoothness prior to network gradients and filters. Also, adding a smoothness prior to the gradient images or filters of convolutional networks may improve their generalization capability.

In sum, our work has revealed several intriguing properties of adversarially-trained networks, providing insights for future designs of classifiers robust to out-of-distribution examples.

Acknowledgement

AN is supported by the National Science Foundation under Grant No. 1850117 and donations from NaphCare Foundation, Adobe Research, and Nvidia.



(a) AlexNet

(b) AlexNet-R

Figure 10: Each 7x7 grid shows the top-49 training-set images that highest activate the center unit in a channel. Each column shows five highest-LoU striped concept channels, each from one AlexNet's conv layer in their original resolutions. From top to bottom, AlexNet-R (b) consistently preferred striped patterns, i.e., edges (conv1), vertical bars (conv2), tools, to grids and zebra (conv5). In contrast, AlexNet striped images (a) are much more diverse, including curly patterns (conv4) and dog faces (conv5).

6. Appendix

A. Convolutional layers used in Network Dissection analysis

For both standard and robust models, we ran NetDissect on 5 convolutional layers in AlexNet (Krizhevsky et al., 2012), 12 in GoogLeNet (Szegedy et al., 2015), and 5 in ResNet-50 architectures (He et al., 2016). For each layer, we use after-ReLU activations (if ReLU exists).

AlexNet layers: conv1, conv2, conv3, conv4, conv5. Refer to these names in Krizhevsky et al. (2012).

GoogLeNet layers: conv1, conv2, conv3, inception3a, inception3b, inception4a, inception4b, inception4c, inception4d, inception4e, inception5a, inception5b

Refer to these names in PyTorch code <https://github.com/pytorch/vision/blob/master/torchvision/models/googlenet.py> L83-L101.

ResNet-50 layers: conv1, layer1, layer2, layer3, layer4

Refer to these names in PyTorch code <https://github.com/pytorch/vision/blob/master/torchvision/models/resnet.py> L145-L155).

B. Kernel smoothness visualization

We visualize the conv1 weights of the 6 models and plot them side by side to compare their kernel smoothness (Fig. A1). The kernels in R models are consistently smoother than its counterpart. For a more straight forward visualization, we use Spearman rank correlation score to pair the similar kernels in AlexNet and AlexNet-R (Fig. A2).

C. Object and color detectors of AlexNet

We compared the layer-wise difference of object and color detectors of AlexNet and AlexNet-R (Fig. A3). We can see in Fig. A3a that AlexNet has more object detectors and fewer color detectors compared to AlexNet-R.

D. Total variance (TV) of AlexNet & AlexNet-R on clean/noisy images

The total variances of AlexNet & AlexNet-R plot (Fig. A4) shows that the early layer i.e. conv1 in AlexNet-R can filter out Gaussian noise. The total variances of clean and noisy input results in similar value in conv1 in AlexNet-R, this means the noise has been filtered by conv1.

E. ImageNet-C evaluation

In Table A1, we evaluate the validation accuracy of 6 models on 15 common types of image corruptions in ImageNet-C. It turns out that shape biased model does not necessary mean better generalization on these image corruptions. But the R models of AlexNet and ResNet do shows better performance in noise and blur distortions.

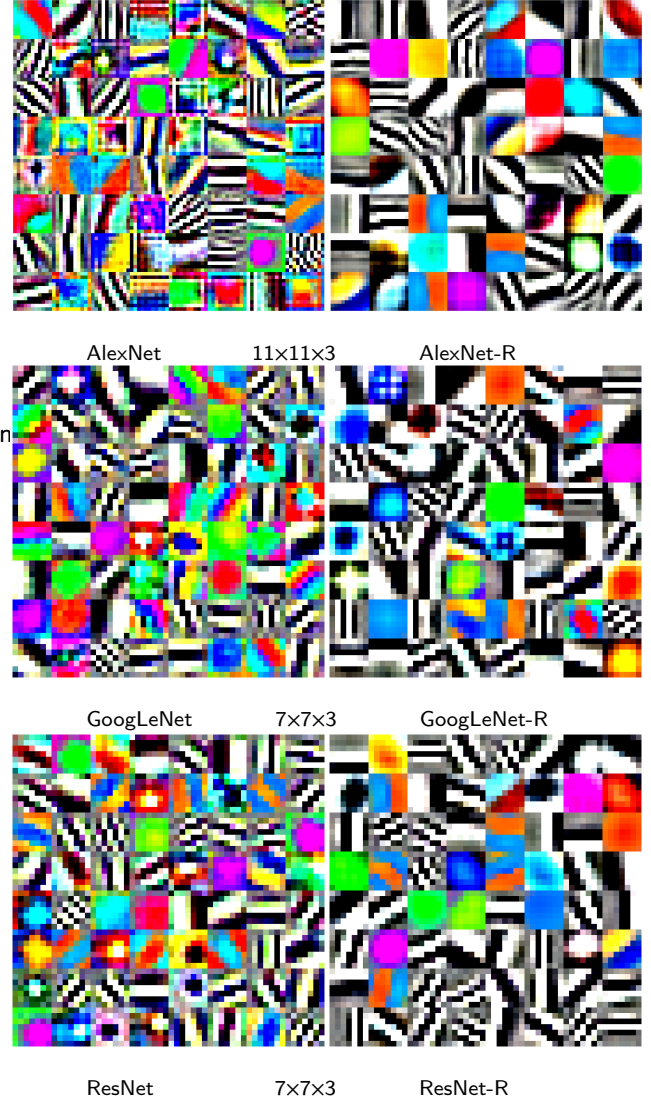


Figure A1: All 64 conv1 filters of in each standard network (left) and its counterpart (right). The filters of R models (right) are smoother and less diverse compared to those in standard models (left). Especially, the edge filters of standard networks are noisier and often contain multiple colors in them.

F. Examples of shape-less and texture-less images

We randomly choose one image in 7 COCO coarser classes (out of 16) and plot the corresponding shape-less and texture-less version (Fig. A5).

G. Visualizing channel preference via cue-conflict and NetDissect

In Fig. A6- A8, we show three samples of the channel preferences experiment. In each of the sample, **Top** is the top-49 images of the channels (Similar to Fig. 10). On the **Middle & Bottom**, we zero-out the corresponding channel and re-run the conflict test to find out the images that were mis-classified. i.e. Fig.A6 the clock images in **Middle**

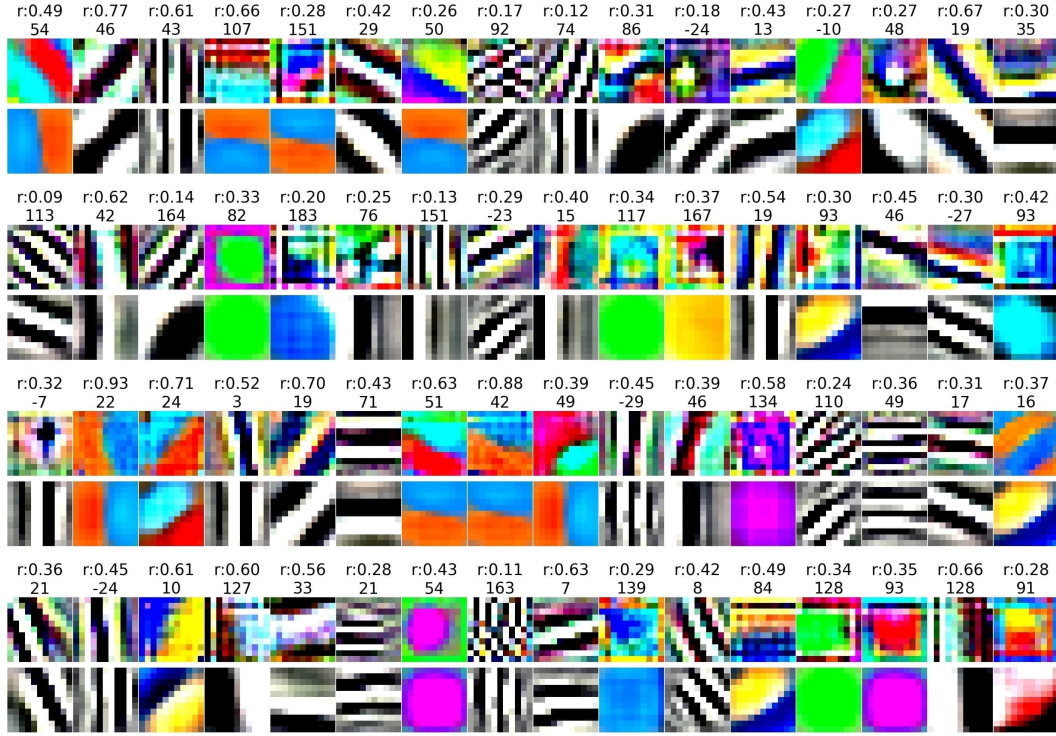
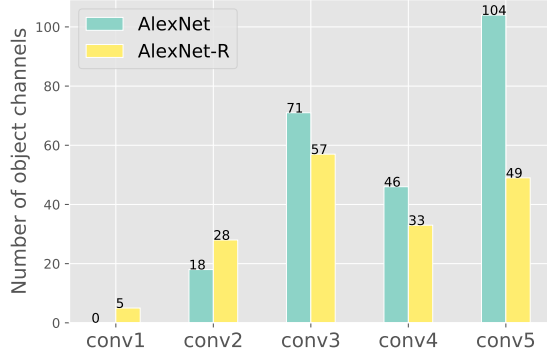


Figure A2: conv1 filters of AlexNet-R are smoother than the filters in standard AlexNet. In each column, we show an AlexNet filter conv1 filter and their nearest filter (bottom) from the AlexNet-R. Above each pair of filters are their Spearman rank correlation score (e.g. $r: 0.36$) and their total variation (TV) difference (i.e. smoothness differences). Standard AlexNet filters are mostly noisier than their nearest R filter (i.e. positive TV differences).

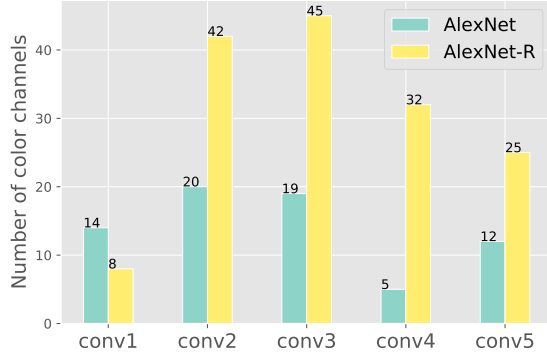
Table A1

Top-1 accuracy of 6 models (in %) on all 15 types of image corruptions in ImageNet-C (Hendrycks and Dietterich, 2019). On average over all 15 distortion types, R models underperform their standard counterparts.

		AlexNet		GoogLeNet		ResNet				
		Standard	Robust	Standard	Robust	Standard	Robust	AdvProp	PGD1	AdvProp PGD5
(a) Noise	Gaussian	11.05	56.10	56.34	26.78	38.43	45.03	49.53		56.39
	Shot	11.15	53.22	50.43	24.66	35.03	44.07	47.56		52.85
	Impulse	8.93	52.49	42.10	24.90	38.40	41.68	49.53		52.39
(b) Blur	Defocus	24.34	28.15	39.63	26.52	43.77	37.95	49.71		56.06
	Glass	22.76	44.50	22.62	43.17	20.71	51.53	30.38		37.74
	Motion	33.87	41.74	44.24	41.25	44.92	50.16	48.27		54.63
	Zoom	38.86	44.27	42.58	43.61	45.16	52.20	49.59		54.97
(c) Weather	Snow	26.59	26.91	52.78	15.60	42.13	40.39	46.01		51.46
	Frost	21.46	13.85	46.14	8.38	37.72	33.51	43.88		50.66
	Fog	27.86	1.64	64.37	12.30	56.78	3.81	54.81		58.64
	Brightness	77.61	62.67	91.60	51.14	85.67	79.44	86.76		88.30
(d) Digital	Contrast	18.24	2.06	78.38	22.63	53.67	3.46	56.57		61.63
	Elastic	75.97	80.98	78.18	77.15	67.86	82.11	74.23		78.44
	Pixelate	57.94	79.46	82.47	79.35	62.40	83.21	67.88		76.38
	JPEG	72.82	85.07	80.27	81.72	73.66	85.51	79.75		82.01
(e) Extra	Speckle Noise	17.55	58.42	51.32	31.31	41.74	52.57	52.80		58.07
	Gaussian Blur	28.68	31.26	45.52	30.36	47.56	41.70	55.68		60.43
	Spatter	28.68	31.26	45.52	30.36	47.56	41.70	55.68		60.43
	Saturate	46.90	63.66	65.36	57.48	58.58	70.72	66.21		71.44
mean Accuracy		37.16	47.34	59.38	40.34	51.70	51.72	57.86		62.80



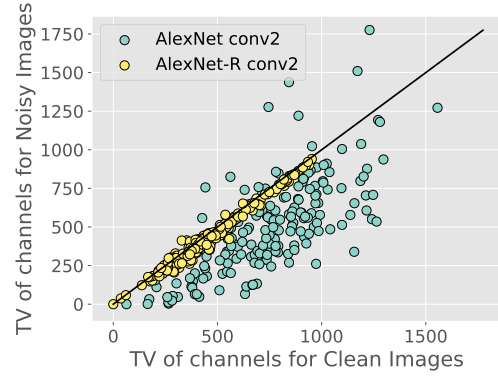
(a) Number of object detectors per AlexNet layer



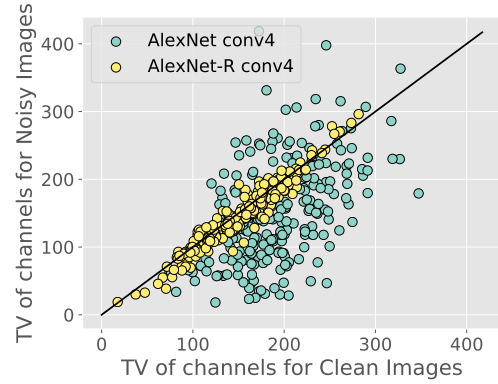
(b) Number of color detectors per AlexNet layer

Figure A3: In higher layers (here, conv4 and conv5), AlexNet-R have fewer object detectors but more color detector units compared to standard AlexNet. The differences between the two networks increase as we go from lower to higher layers. Because both networks share an identical architecture, the plots here demonstrate a substantial shift in the functionality of the neurons as the result of adversarial training—detecting more colors and textures and fewer objects. Similar trends were also observed between standard and R models of GoogLeNet and ResNet-50 architectures.

were classified into shape category by cue-conflict test. After zeroing-out the channel, the network lose the ability to classify the image into shape category.



(a) conv2



(b) conv4

Figure A4: Each point shows the Total Variation (TV) of the activation maps on clean and noisy images for an AlexNet or AlexNet-R channel. We observe a striking difference in conv1: The smoothness of R channels remains unchanged before and after noise addition, explaining their superior performance in classifying noisy images. While the channel smoothness differences (between two networks) are gradually smaller in higher layers, we still observe R channels are consistently smoother.

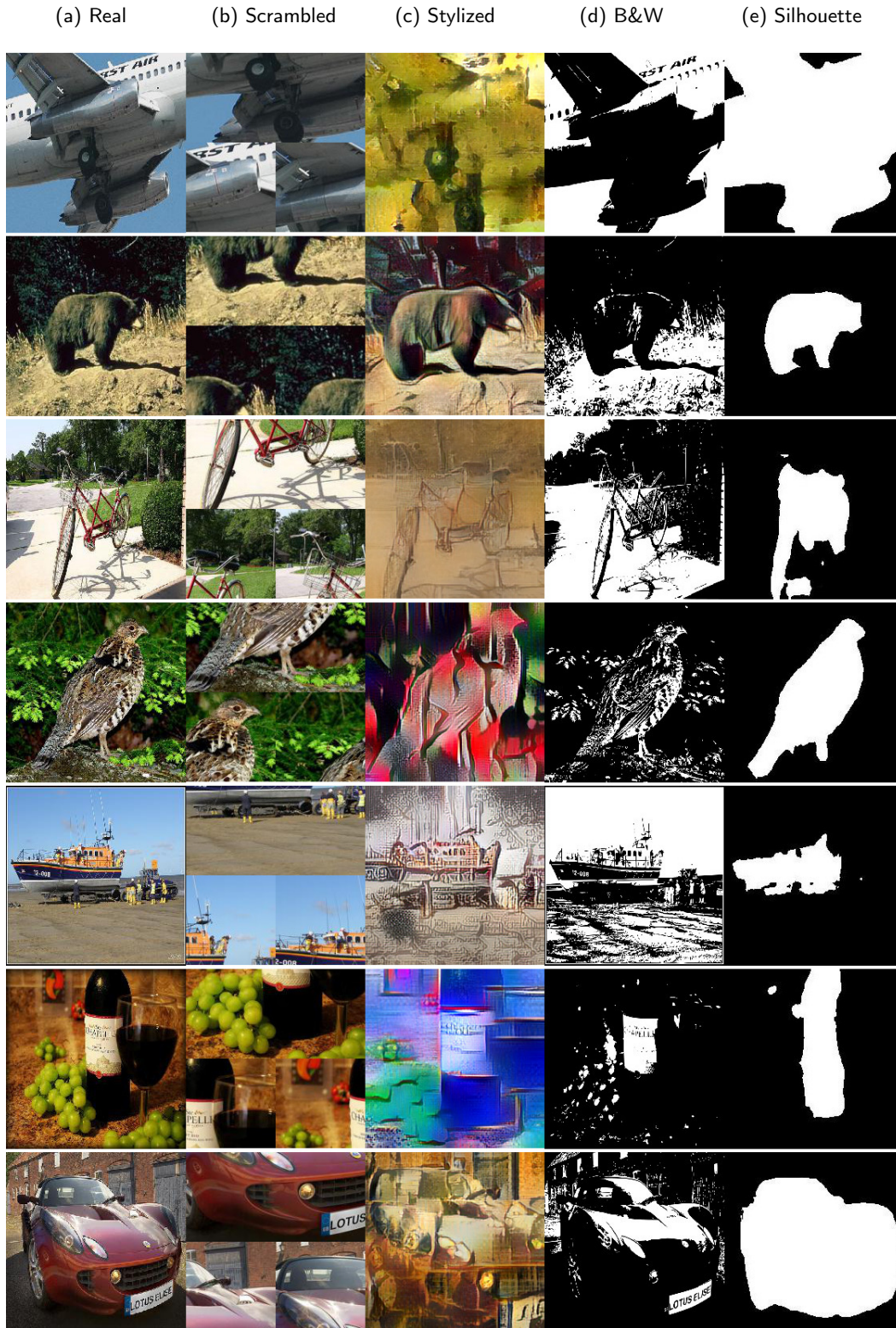


Figure A5: Applying different transformation that remove shape/texture on real images. We randomly show an example of 7 out of 16 COCO coarser classes. See Table 3 for classification accuracy scores on different images distortion dataset in 1000 classes (Except for Silhouette). **Note: Silhouette are validate in 16 COCO coarse classes.*

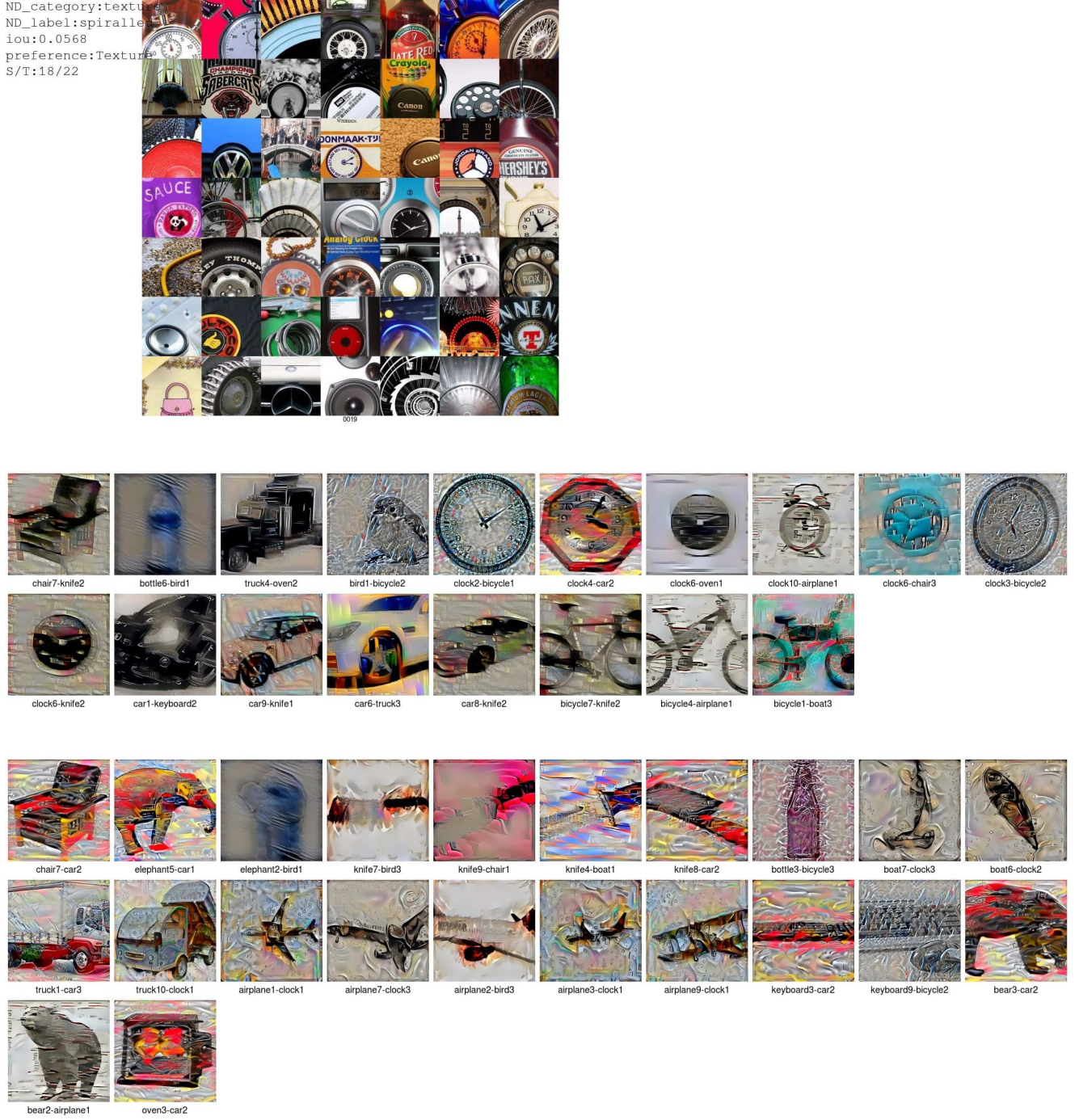


Figure A6: AlexNet conv4₁₉ with Shape and Texture scores of 18 and 22, respectively. It has a NetDissect label of spiralled (IoU: 0.0568) under texture category. Although this neuron is in NetDissect texture category, the misclassified images suggest that this neuron helps in both shape- and texture-based recognition. **Top:** Top-49 images that highest-activated this channel. **Middle:** Mis-classified images in shape category (18 images). **Bottom:** Mis-classified images in texture category (22 images).

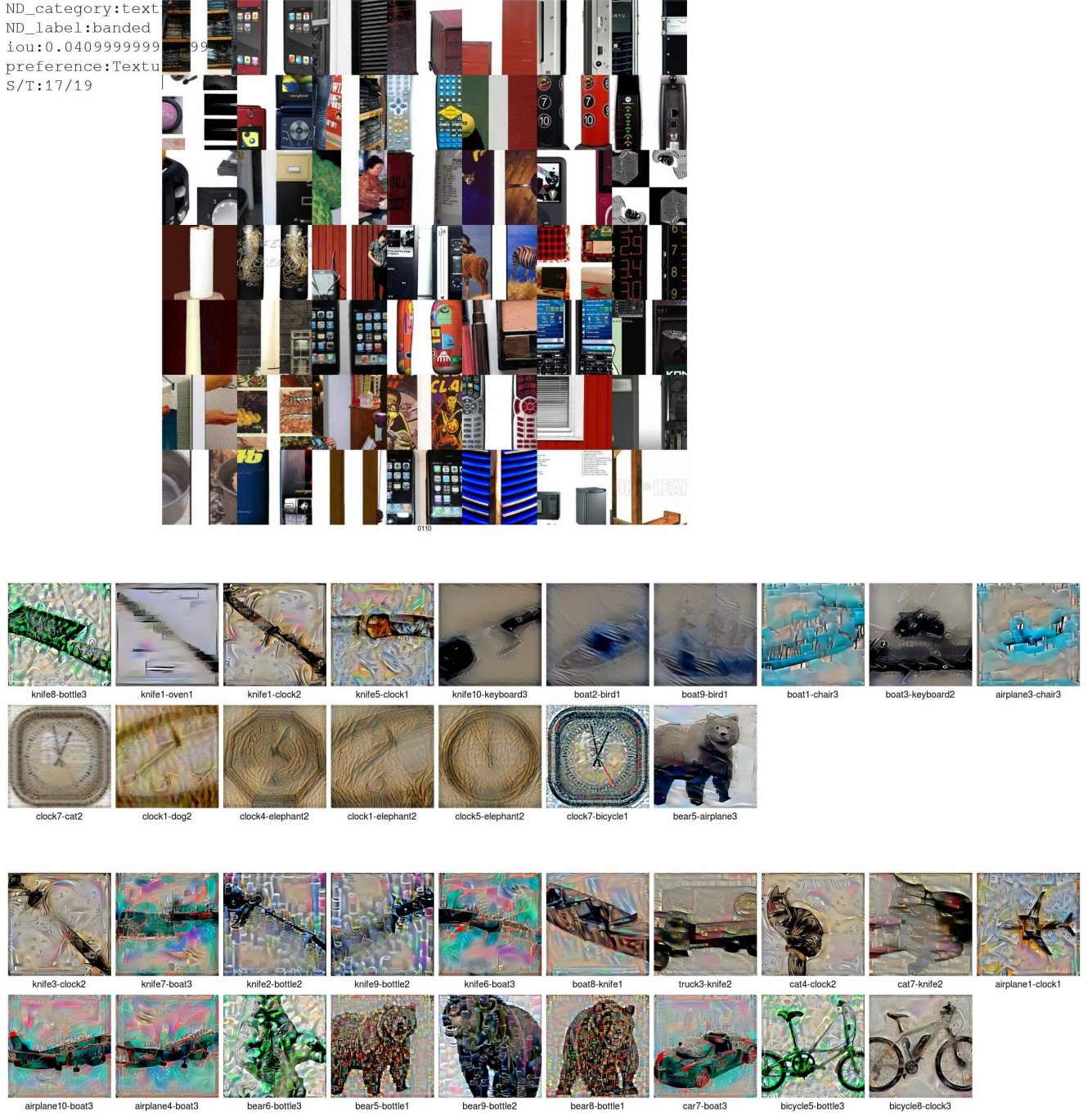


Figure A7: AlexNet-R conv5₁₁₀ with Shape and Texture scores of 17 and 19, respectively. It has a NetDissect label of banded (IoU: 0.0409) under texture category. This neuron has almost equal Shape and Texture scores and is useful in detecting both the shape and textures of knives and bottles at the same time. **Top:** Top-49 images that highest-activated this channel. **Middle:** Mis-classified images in shape category. **Bottom:** Mis-classified images in texture category.

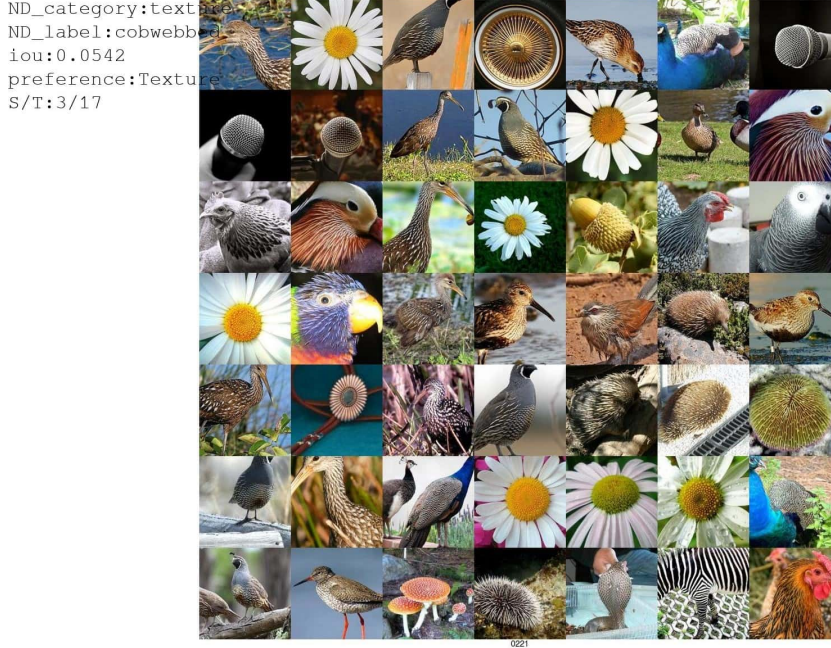
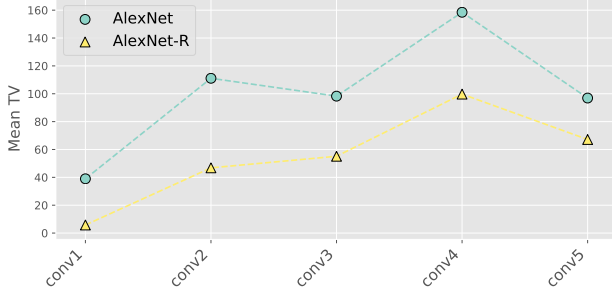
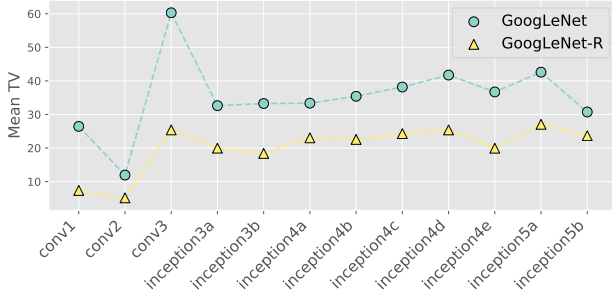


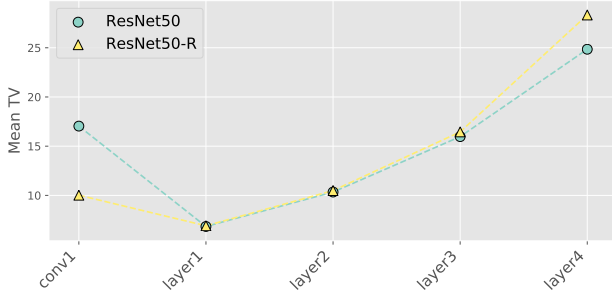
Figure A8: AlexNet conv5₂₂₁ with Shape and Texture scores of 3 and 17, respectively. It has a NetDissect label of cobwebbed (IoU: 0.0542) under texture category. This is a heavily texture-biased neuron that helps networks detect animals by their fur textures. **Top:** Top-49 images that highest-activated this channel. **Middle:** Mis-classified images in shape category. **Bottom:** Mis-classified images in texture category.



(a) Mean layer-wise kernel TV of AlexNet and AlexNet-R

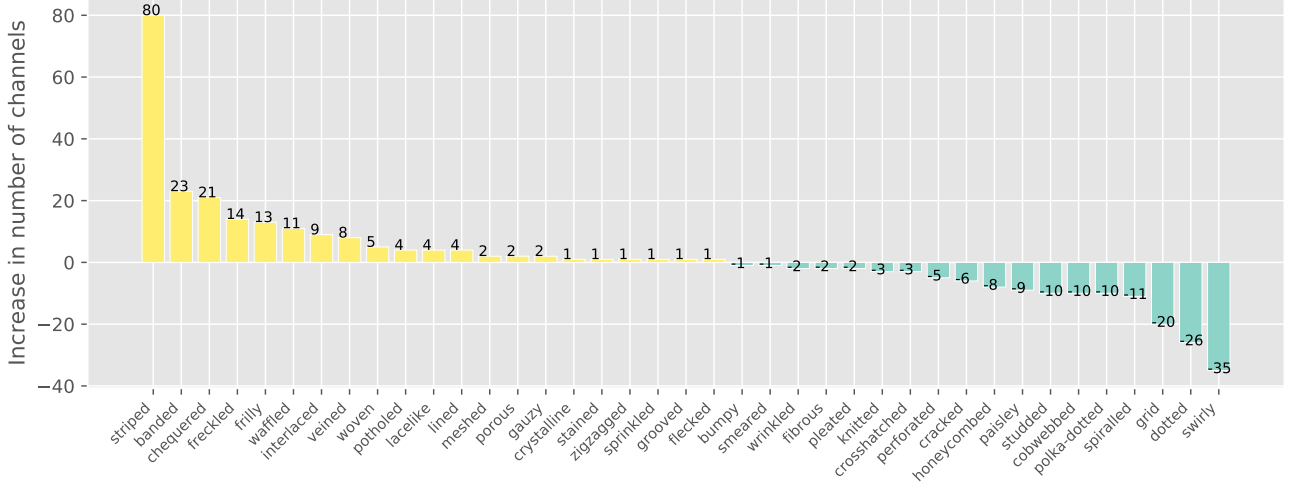


(b) Mean layer-wise kernel TV of GoogLeNet and GoogLeNet-R

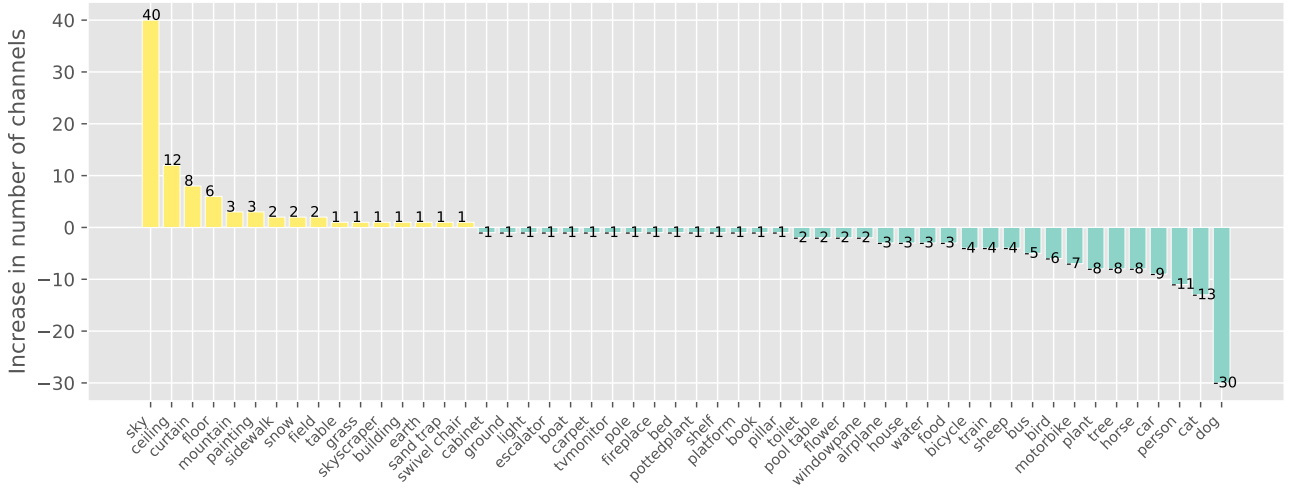


(c) Mean layer-wise kernel TV of ResNet and ResNet-R

Figure A9: For all main conv layers, AlexNet-R filters are smoother (i.e. lower TV mean) than their counterparts in AlexNet (a). The same observation was found in GoogLeNet-R vs. GoogLeNet comparison (b). In ResNet-R, its early filters at conv1 are also smoother than those in ResNet.



(a) Differences in texture channels between AlexNet and AlexNet-R



(b) Differences in object channels between AlexNet and AlexNet-R

Figure A10: In each bar plot, we column shows the difference in the number of channels (between AlexNet-R and AlexNet) for a given concept e.g. striped or banded. That is, yellow bars (i.e. positive numbers) show the count of channels that the R model has more than the standard network in the same concept. Vice versa, teal bars represent the concepts that R models have fewer channels. The NetDissect concept names are given in the x-axis. **Top:** In the texture category, the R model has a lot more simple texture patterns e.g. striped and banded (see Fig. A11 for example patterns in these concepts). **Bottom:** In the object category, AlexNet-R often prefers simpler-object detectors e.g. sky or ceiling (Fig. A10b; leftmost) while the standard network has more complex-objects detectors e.g. dog and cat (Fig. A10b; rightmost).

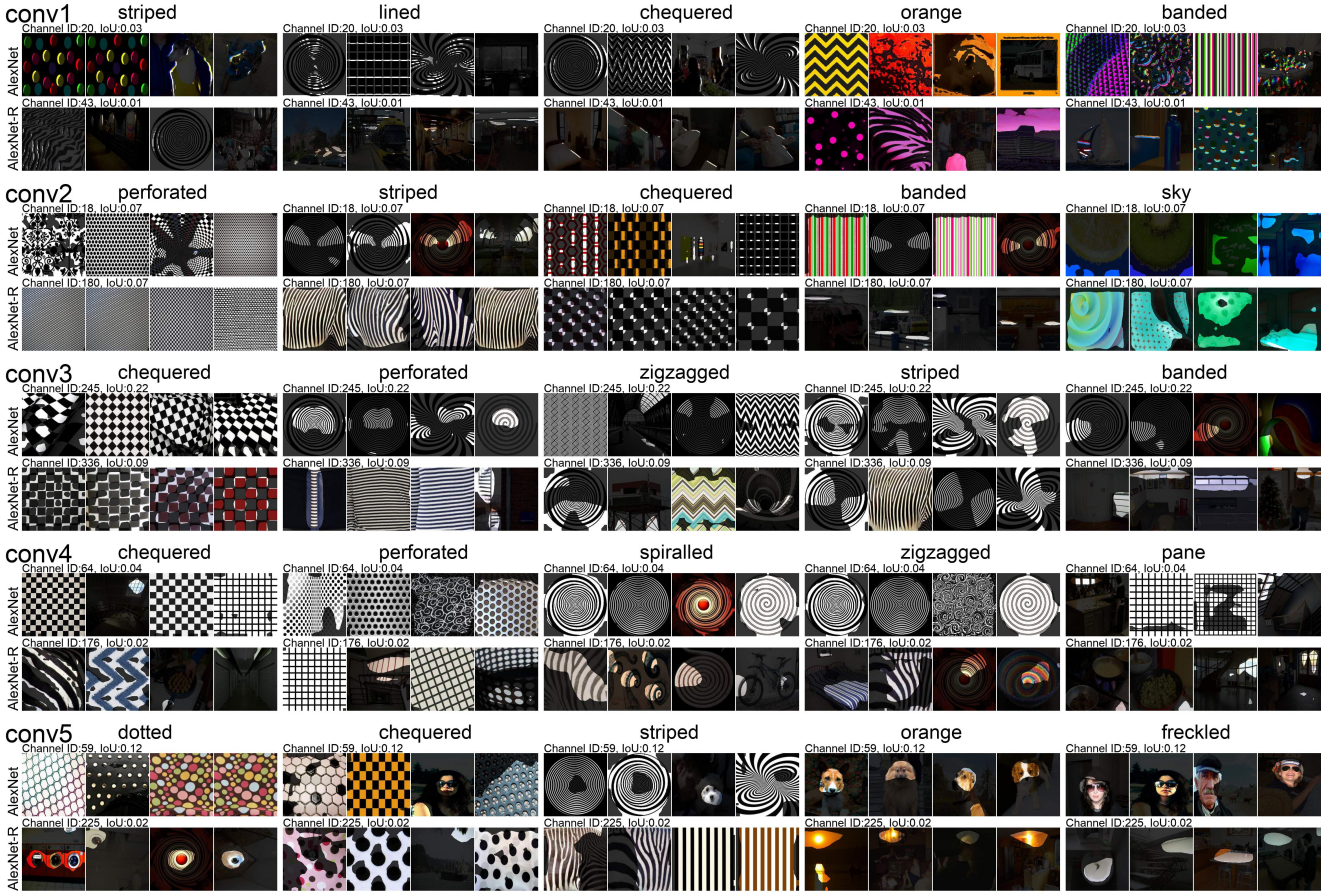
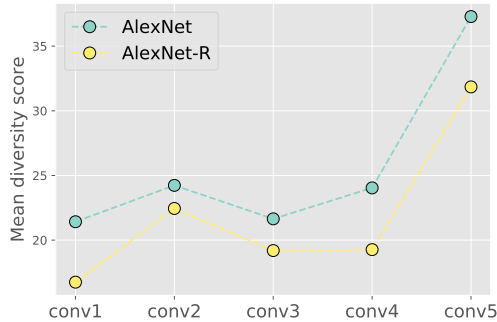
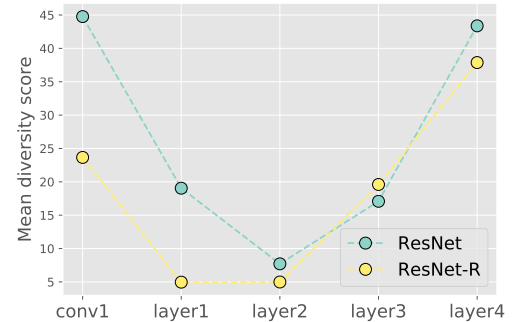


Figure A11: The NetDissect images preferred by the channels in the top-5 most important concepts in AlexNet (i.e. highest accuracy drop when zeroed out; see Sec. 3.3.2). For each concept, we show the highest-IoU channels.



(a) AlexNet layer-wise mean diversity



(b) ResNet layer-wise mean diversity

Figure A12: In each plot, we show the mean diversity scores across all channels in each layer. Both AlexNet-R and ResNet-R consistently have channels with lower diversity scores (i.e. detecting fewer unique concepts) than the standard counterparts.

References

- Arpit, D., Jastrzebski, S., Ballas, N., Krueger, D., Bengio, E., Kanwal, M. S., Maharaj, T., Fischer, A., Courville, A., Bengio, Y., et al. (2017). A closer look at memorization in deep networks. In *Proceedings of the 34th International Conference on Machine Learning-Volume 70*, pages 233–242. JMLR. org.
- Bansal, N., Agarwal, C., and Nguyen, A. (2020). Sam: The sensitivity of attribution methods to hyperparameters. In *Proceedings of the IEEE/CVF conference on computer vision and pattern recognition*, pages 8673–8683.
- Bau, D., Zhou, B., Khosla, A., Oliva, A., and Torralba, A. (2017). Network dissection: Quantifying interpretability of deep visual representations. In *Proceedings of the IEEE conference on computer vision and pattern recognition*, pages 6541–6549.
- Brendel, W. and Bethge, M. (2019). Approximating cnns with bag-of-local-features models works surprisingly well on imagenet. *International Conference on Learning Representations*.
- Caesar, H., Uijlings, J., and Ferrari, V. (2018). Coco-stuff: Thing and stuff classes in context. In *Proceedings of the IEEE Conference on Computer Vision and Pattern Recognition*, pages 1209–1218.
- Chen, L.-C., Papandreou, G., Kokkinos, I., Murphy, K., and Yuille, A. L. (2017). Deeplab: Semantic image segmentation with deep convolutional nets, atrous convolution, and fully connected crfs. *IEEE transactions on pattern analysis and machine intelligence*, 40(4):834–848.
- Cichy, R. M., Khosla, A., Pantazis, D., Torralba, A., and Oliva, A. (2016). Comparison of deep neural networks to spatio-temporal cortical dynamics of human visual object recognition reveals hierarchical correspondence. *Scientific reports*, 6(1):1–13.
- De Palma, G., Kiani, B., and Lloyd, S. (2019). Random deep neural networks are biased towards simple functions. In *Advances in Neural Information Processing Systems*, pages 1962–1974.
- Engstrom, L., Ilyas, A., Santurkar, S., and Tsipras, D. (2019). Robustness (python library).
- Engstrom, L., Ilyas, A., Santurkar, S., Tsipras, D., Tran, B., and Madry, A. (2020). Adversarial robustness as a prior for learned representations.
- Ford, N., Gilmer, J., and Cubuk, E. D. (2019). Adversarial examples are a natural consequence of test error in noise.
- Gatys, L. A., Ecker, A. S., and Bethge, M. (2016). Image style transfer using convolutional neural networks. In *Proceedings of the IEEE conference on computer vision and pattern recognition*, pages 2414–2423.
- Geirhos, R., Rubisch, P., Michaelis, C., Bethge, M., Wichmann, F. A., and Brendel, W. (2019). Imagenet-trained CNNs are biased towards texture; increasing shape bias improves accuracy and robustness. In *International Conference on Learning Representations*.
- Geirhos, R., Temme, C. R., Rauber, J., Schütt, H. H., Bethge, M., and Wichmann, F. A. (2018). Generalisation in humans and deep neural networks. In *Advances in Neural Information Processing Systems*, pages 7538–7550.
- Gilmer, J., Ford, N., Carlini, N., and Cubuk, E. (2019). Adversarial examples are a natural consequence of test error in noise. In *International Conference on Machine Learning*, pages 2280–2289.
- He, K., Zhang, X., Ren, S., and Sun, J. (2016). Deep residual learning for image recognition. In *Proceedings of the IEEE conference on computer vision and pattern recognition*, pages 770–778.
- Hendrycks, D. and Dietterich, T. (2019). Benchmarking neural network robustness to common corruptions and perturbations. In *International Conference on Learning Representations*.
- ImageMagick (2020). Imagemagick.
- Krizhevsky, A., Sutskever, I., and Hinton, G. E. (2012). Imagenet classification with deep convolutional neural networks. In *Advances in neural information processing systems*, pages 1097–1105.
- Madry, A., Makelov, A., Schmidt, L., Tsipras, D., and Vladu, A. (2018). Towards deep learning models resistant to adversarial attacks. In *International Conference on Learning Representations*.
- Nguyen, A., Dosovitskiy, A., Yosinski, J., Brox, T., and Clune, J. (2016a). Synthesizing the preferred inputs for neurons in neural networks via deep generator networks. In *Advances in neural information processing systems*, pages 3387–3395.
- Nguyen, A., Yosinski, J., and Clune, J. (2016b). Multifaceted feature visualization: Uncovering the different types of features learned by each neuron in deep neural networks. In *Visualization for Deep Learning Workshop, ICML conference*.
- Nguyen, A., Yosinski, J., and Clune, J. (2019). Understanding neural networks via feature visualization: A survey. In *Explainable AI: Interpreting, Explaining and Visualizing Deep Learning*, pages 55–76. Springer.
- PyTorch (2019). torchvision.models — pytorch master documentation. <https://pytorch.org/docs/stable/torchvision/models.html>. (Accessed on 09/21/2019).
- Rahaman, N., Baratin, A., Arpit, D., Dräxler, F., Lin, M., Hamprecht, F. A., Bengio, Y., and Courville, A. C. (2019). On the spectral bias of neural networks. In *ICML*, pages 5301–5310.
- Rajalingham, R., Issa, E. B., Bashivan, P., Kar, K., Schmidt, K., and Di-Carlo, J. J. (2018). Large-scale, high-resolution comparison of the core visual object recognition behavior of humans, monkeys, and state-of-the-art deep artificial neural networks. *Journal of Neuroscience*, 38(33):7255–7269.
- Rozsa, A. and Boulton, T. E. (2019). Improved adversarial robustness by reducing open space risk via tent activations. *arXiv preprint arXiv:1908.02435*.
- Rudin, L. I., Osher, S., and Fatemi, E. (1992). Nonlinear total variation based noise removal algorithms. *Physica D: nonlinear phenomena*, 60(1-4):259–268.
- Russakovsky, O., Deng, J., Su, H., Krause, J., Satheesh, S., Ma, S., Huang, Z., Karpathy, A., Khosla, A., Bernstein, M., et al. (2015). Imagenet large scale visual recognition challenge. *International journal of computer vision*, 115(3):211–252.
- Salman, H., Ilyas, A., Engstrom, L., Kapoor, A., and Madry, A. (2020). Do adversarially robust imagenet models transfer better? *Advances in Neural Information Processing Systems*, 33.
- Santurkar, S., Ilyas, A., Tsipras, D., Engstrom, L., Tran, B., and Madry, A. (2019). Image synthesis with a single (robust) classifier. In Wallach, H., Larochelle, H., Beygelzimer, A., d'Alché-Buc, F., Fox, E., and Garnett, R., editors, *Advances in Neural Information Processing Systems*, volume 32, pages 1262–1273. Curran Associates, Inc.
- Serre, T. (2019). Deep learning: the good, the bad, and the ugly. *Annual review of vision science*, 5:399–426.
- Szegedy, C., Liu, W., Jia, Y., Sermanet, P., Reed, S., Anguelov, D., Erhan, D., Vanhoucke, V., and Rabinovich, A. (2015). Going deeper with convolutions. In *Proceedings of the IEEE conference on computer vision and pattern recognition*, pages 1–9.
- Szegedy, C., Zaremba, W., Sutskever, I., Bruna, J., Erhan, D., Goodfellow, I., and Fergus, R. (2014). Intriguing properties of neural networks. In *International Conference on Learning Representations*.
- Tsipras, D., Santurkar, S., Engstrom, L., Turner, A., and Madry, A. (2019). Robustness may be at odds with accuracy. In *International Conference on Learning Representations*.
- Valle-Perez, G., Camargo, C. Q., and Louis, A. A. (2019). Deep learning generalizes because the parameter-function map is biased towards simple functions. In *International Conference on Learning Representations*.
- Xie, C., Tan, M., Gong, B., Wang, J., Yuille, A. L., and Le, Q. V. (2020). Adversarial examples improve image recognition. In *Proceedings of the IEEE/CVF Conference on Computer Vision and Pattern Recognition*, pages 819–828.
- Xie, C. and Yuille, A. (2020). Intriguing properties of adversarial training at scale. In *International Conference on Learning Representations*.
- Yin, D., Gontijo Lopes, R., Shlens, J., Cubuk, E. D., and Gilmer, J. (2019). A fourier perspective on model robustness in computer vision. *Advances in Neural Information Processing Systems*, 32:13276–13286.
- Yosinski, J., Clune, J., Bengio, Y., and Lipson, H. (2014). How transferable are features in deep neural networks? In *Advances in Neural Information Processing Systems*, pages 3320–3328.
- Zhang, T. and Zhu, Z. (2019). Interpreting adversarially trained convolutional neural networks. In *International Conference in Machine Learning*.